DOI: http://dx.doi.org/10.15446/ing.investig.v39n2.76586

# Effect of the presence of $CuO_x$ on the catalytic behavior of bimetallic Au-Cu catalyst supported on Ce-Zr mixed oxide in CO preferential oxidation

## Influencia de la presencia de $CuO_x$ sobre el comportamiento catalítico de un catalizador bimetálico Au-Cu soportado en óxido mixto Ce-Zr en la oxidación preferencial de CO

Juan David Arévalo[1], Julio César Vargas[2], and Luis Fernando Córdoba[3]


### ABSTRACT

The effect of the presence of copper was evaluated on a bimetallic catalyst Au-Cu based on mixed oxide cerium-zirconium in the preferential oxidation of CO (CO-PROX). Six catalytic materials, based on mixed oxides, were prepared: (1) the support (CeZr); the monometallic catalysts, i.e. (2) gold (Au/CeZr), (3) impregnated copper oxide ($CuO_x$/CeZr) and (4) incorporated copper (CuCeZr); and the bimetallic catalysts, i.e. (5) impregnated copper oxide and gold (Au-$CuO_x$/CeZr), and (6) gold and incorporated copper (Au/CuCeZr). The catalysts were evaluated in the CO-PROX in the range 30-300 °C and atmospheric pressure, where the Au-$CuO_x$/CeZr showed the best catalytic behavior. The influence of $CO_2$ and $H_2O$ in the feed stream was evaluated on the catalytic performance of the Au-$CuO_x$/CeZr. An inhibitory effect for the $CO_2$ was observed, while the presence of $H_2O$ enhanced the performance. Additionally, the catalytic stability was evaluated, reaching CO conversion of 93 % and selectivity of 90 % for 118 h. The catalytic materials were characterized by XRD, showing in all cases the fluorite cubic structure. The $N_2$ adsorption-desorption analyses showed that synthesized materials were mesoporous and the TPR-$H_2$ test reveals that the presence of the active phase increases the reducibility of $Ce^{4+}$ to $Ce^{3+}$. Reduction peaks of the gold catalyst were present at lower temperatures than those of the copper catalyst, which is related to a hydrogen spillover phenomenon. Finally, the samples were analyzed by SEM and TEM, which confirmed the formation of nano-particles with a diameter of about 4 nm.


**Keywords:** Preferential oxidation of CO, Nano-gold particles, Copper, Bimetallic Au-Cu, Mixed oxide.


### RESUMEN

El efecto de la presencia de cobre en catalizadores bimetálicos Au-Cu a base de óxidos mixtos de cerio-zirconio fue evaluado en la oxidación preferencial de CO (CO-PROX). Se prepararon seis materiales catalíticos: (1) el soporte (CeZr); los catalizadores monometálicos que fueron (2) oro (Au/CeZr), (3) cobre impregnado ($CuO_x$/CeZr) y (4) cobre incorporado (CuCeZr); y los catalizadores bimetálicos que fueron (5) óxido de cobre impregnado y oro (Au-$CuO_x$/CeZr), y (6) oro y cobre incorporado (Au/CuCeZr). Los catalizadores se evaluaron en el CO-PROX en un rango de temperaturas de 30-300 °C y presión atmosférica, donde el Au-$CuO_x$/CeZr mostró el mejor desempeño catalítico. Se evaluó la influencia de $CO_2$ y $H_2O$ en la mezcla de alimento sobre el desempeño del catalizador Au-$CuO_x$/CeZr, donde se observó un efecto inhibitorio del $CO_2$, mientras que la presencia del agua mejoró el desempeño. Adicionalmente, se evaluó la estabilidad catalítica, la cual alcanzó conversiones de CO de 93 % con una selectividad de 90 %, durante 118 h. Los materiales catalíticos se caracterizaron por DRX, presentando en todos los casos la estructura fluorita cúbica. Las pruebas de adsorción y desorción de $N_2$ mostraron que los materiales sintetizados eran mesoporosos. Los ensayos de TPR-$H_2$, mostraron que la presencia de la fase activa incrementó la reducibilidad de $Ce^{4+}$ a $Ce^{3+}$. Los picos de reducción del catalizador de oro se presentaron a temperaturas más bajas con respecto al catalizador de cobre, lo cual se relaciona con el fenómeno *spillover* para el hidrógeno. Finalmente, las muestras se analizaron por SEM y TEM, las cuales confirmaron la formación de nanopartículas con un diámetro alrededor de 4nm.


**Palabras clave:** Oxidación preferencial de CO, Nanopartículas de oro, Cobre, Óxido mixto.

**Received:** December 3rd, 2018
**Accepted:** April 22nd, 2019

[1]Chemical Engineer, Universidad Nacional de Colombia, Colombia. Affiliation: Postgraduate student in Chemical Engineering, Universidad Nacional de Colombia, Colombia. E-mail: jdarevaloa@unal.edu.co.
[2]Chemical Engineer, Universidad Nacional de Colombia, Colombia. M.Sc. and Ph.D. in Chemical Engineering, Universidad Nacional de Colombia, Colombia. Ph.D. in Chemistry, Université de Strasbourg I -Louis Pasteur, France. Affiliation: Full-Professor, Universidad Nacional de Colombia, Colombia. E-mail: jcvargass@unal.edu.co.
[3]Chemical Engineer, Universidad de Antioquia, Colombia. M.Sc. and Ph.D. in Chemical Sciences, Universidad de Antioquia, Colombia. Affiliation: Associate Professor, Universidad Nacional de Colombia, Colombia.
E-mail: lfcordobac@unal.edu.co.

**How to cite:** Arévalo, J. D., Vargas, J. C., and Córdoba, L. F. (2019). Effect of the presence of $CuO_x$ on the catalytic behavior of bimetallic Au-Cu catalyst supported on Ce-Zr mixed oxide in CO preferential oxidation. *Ingeniería e Investigación*, 39(2), 21-30. DOI: 10.15446/ing.investig.v39n2.76586

## Introduction

Proton Exchange Membrane Fuel Cells (PEMFC) are very interesting in portable applications, since they generate energy from hydrogen with high efficiency, reduced emissions and quick responses to charge changes (Salemme, Menna, Simeone and Volpicelli, 2010). The production of $H_2$ for PEMFC is usually accomplished by multistep processes that include catalytic reforming of hydrocarbons or oxygenated hydrocarbons followed by water–gas shift (WGS) reaction (Martínez-Arias, Hungría and Munuera, 2006). However, the gas stream obtained from these processes contains, in most cases, small amounts of CO and $H_2O$. The PEMFC have low tolerance to CO (10 ppm), due to the poisoning by CO adsorption on the cell Pt anode. For this reason and for the effect on the kinetic of oxidation, there is a limitation to expand their use (Cheng et al., 2007; Choudhary and Goodman, 2002; Ko et al., 2006).

Several methods have been reported for carbon monoxide removal from the steam reforming stream, such as preferential oxidation of CO (CO-PROX), selective methanation of CO, and selective diffusion through membranes (Haryanto, Fernando, Murali and Adhikari, 2005; Manzolini and Tosti, 2008; Ocampo, Louis and Roger, 2009). Among these, preferential oxidation of CO (CO-PROX) is the simplest and most direct and accessible method for removing CO (Avgouropoulos et al., 2002; Epling, Cheekatamarla and Lane, 2003).

Cerium oxide ($CeO_2$) has been broadly reported to be an active support and promotor for the synthesis of oxidation catalysts due to its structural properties (Fonseca, Royer, et al., 2012) and redox behavior that allows high oxygen mobility and storage, thus enhancing oxygen exchange with the reaction environment (Laguna et al., 2010; Trovalleri, 2002). Additionally, it has been found that the addition of $ZrO_2$ improves the thermal stability and the redox properties of $CeO_2$. It also improves oxygen mobility due to the formation of a mixed oxide system that promotes electronic distortions in the oxide framework, which contributes to the homogeneous dispersion of the deposited metal, long-term stability of the catalyst and an increase in the resistance to high temperatures, avoiding sintering problems (Biswas and Kunzru, 2008; Das et al., 2015).

In CO-PROX, gold supported catalysts in form of nanoparticles present better catalytic performance. Compared with other noble metals, Au catalysts are more active and selective for CO oxidation than for $H_2$ oxidation (Choudhary and Goodman, 2002; Haruta, 2002). Thus, the high dispersion of nano-gold particles provides a suitable catalytic activity in CO oxidation (Haruta, Kobayashi, Sano and Yamada, 1987). Gold supported on cerium oxide catalyst has been studied for the CO-PROX process due to its capacity to store and provide oxygens in the reaction of CO oxidation (Fonseca, Royer, et al., 2012). However, this catalysts can present the drawback of poor resistance to the presence of $CO_2$ in the reactant mixture (Trovalleri, 2002).

Recently, copper-based catalytic systems have emerged as promising substitutes for such noble metal catalysts, especially with $CeO_2$ as support, thanks to their low cost, high catalytic performance and high selectivity of $O_2$ to $CO_2$ (W. Liu and Flytzanistephanopoulos, 1995; Martínez-Arias et al., 2003). The excellent catalytic performance of $CuO/CeO_2$ catalyst is on account of the high oxygen storage/release capability of $CeO_2$ via the redox couple $Ce^{4+}/Ce^{3+}$ and the strong interaction between CuO and $CeO_2$ (Kosmambetova et al., 2010). Mariño et al. (2008) concluded that the activity of copper and cerium oxides was lower when evaluated separately. However, the catalyst prepared with both oxides presented a high performance in the CO-PROX.

For $CuO_x/CeO_2$ catalysts, numerous preparation methods have been described in the literature, including co-precipitation, impregnation, inert gas condensation, and citric acid complexation–combustion (Di Benedetto, Landi and Lisi, 2018; Marbán and Fuertes, 2005; Zhu et al., 2017). In all cases, nano-sized crystals powders have been obtained.

The cooperative effect of the bimetallic gold and copper oxide has been studied to find an efficient catalyst in the CO-PROX, showing that bimetallic catalysts present better activity and selectivity than monometallic ones. Combining the catalytic properties of both metals has shown an intermediate behavior with good activity (98 % to 80 °C) and selectivity (65 % at 80 °C) (Fonseca, Ferreira, et al., 2012). Consequently, bimetallic gold–copper oxide supported catalyst has been studied in the CO-PROX reaction. Mozer, Dziuba, Vieira and Passos (2009) prepared the bimetallic Au-Cu catalyst on alumina and concluded that the addition of copper increased the selectivity to CO oxidation and reduced the $H_2$ consumption. Liu, Wang, Zhang, Su and Mou (2011) studied bimetallic Au-Cu catalysts over silica and reported a higher catalytic activity than in monometallic catalysts. They also observed the presence of highly disperse nanoparticles on the support with significantly lower particle size. Li et al. (2012) evaluated bimetallic catalysts of gold and copper oxide over mesoporous silica Au-CuO/SBA-15. However, this catalyst is deactivated easily due to both ambient condition and high temperatures.

Laguna et al. (2012) studied catalysts $CuO_x/CeO_2$ and Au-$CuO_x/CeO_2$ (10 % w/w copper and 1 % w/w gold), which presented a better catalytic activity than monometallic catalysts of copper. In contrast, Reina, Ivanova, Laguna, Centeno and Odriozola (2016) concluded that the addition of gold (2 % w/w) in the system $Cu/CeO_2$ with 15 % w/w of copper incorporated in the support do not promote the catalyst activity, due to the high load of the active phase.

Due to the complexity of some of the preparation methods above mentioned, it becomes necessary to search for simplest recipes directed to the potential mass-scale fabrication of the catalyst. The present study proposes to evaluate the cooperative effect between gold and copper oxide supported on cerium-zirconium mixed oxides in the CO-PROX reaction. Two bimetallic catalysts were prepared: one by incipient wetness impregnation to disperse copper over a previous gold supported on cerium-zirconium mixed oxide and another

using copper incorporated in cerium-zirconium oxide support, where the addition of gold was made by co-precipitation.

## Materials and methods

### *Catalyst preparation*

Six catalytic materials were prepared to be evaluated in the CO-PROX reaction: (1) cerium-zirconium mixed oxide support (CeZr), (2) gold on cerium–zirconium mixed oxide (Au/CeZr), (3) impregnated copper on cerium–zirconium mixed oxide ($CuO_x$/CeZr), (4) copper incorporated into cerium–zirconium mixed oxide (CuCeZr), (5) bimetallic catalyst Au-$CuO_x$ with impregnated copper oxide (Au-$CuO_x$/CeZr) and (6) bimetallic catalyst Au-$CuO_x$ with incorporated copper (Au/CuCeZr).

The cerium-zirconium mixed oxide support (CeZr) and the copper incorporated into cerium-zirconium mixed oxide (CuCeZr) were prepared using the pseudo sol-gel like method (Vargas, Libs, Roger and Kiennemann, 2005), based on the thermal decomposition of propionate precursors. The starting materials were cerium (III) acetate hydrate (99,9 %, Sigma-Aldrich), zirconium (IV) acetylacetonate (98 %, Sigma-Aldrich) and copper (II) acetate monohydrate (99,5 %, Sigma-Aldrich). The salts were dissolved separately in propionic acid (99,5 %, Sigma-Aldrich) under ebullition, mixed during 1 h, and then carried to controlled evaporation under vacuum pressure. The resin obtained was calcined at 550 °C for 6 hours.

The addition of gold was made following the methodology reported by Lin and Wan (2003). A suitable amount of tetrachloroauric acid trihydrate (≥ 99,9 %, Sigma Aldrich) was dissolved in 250 ml of distillated water and then, a solution of sodium hydroxide (97,0 %, Merck) was added for adjusting the pH solution to 6. After that, the support material (CeZr or CuCeZr) was mixed with the gold solution and stirred for six hours at ambient temperature. After filtration and washing, the solid was carried-out to calcination at 350 °C for 8 hours. The samples obtained were gold on cerium–zirconium mixed oxide (Au/CeZr) and bimetallic catalyst Au-$CuO_x$ with incorporated copper (Au/CuCeZr).

The monometallic and bimetallic catalysts impregnated with copper were prepared using incipient wetness impregnation method (Fonseca et al., 2012). Copper nitrate trihydrate (Chemi) was dissolved in distillated water, then added over the catalytic material (CeZr or Au/CeZr) with uniform mixing at ambient temperature. Finally, the mixture was carried to calcination at 350 °C for 8 hours. The samples obtained were impregnated copper oxide on cerium-zirconium mixed oxide ($CuO_x$/CeZr) and bimetallic catalyst Au-$CuO_x$ over cerium-zirconium mixed oxide (Au-$CuO_x$/CeZr).

### *Catalyst characterization*

The specific surface area was determined from $N_2$ adsorption/desorption isotherms using the BET method in an Autosorb-1 Quantachrome. The metallic composition was determined by atomic absorption spectrophotometry (GBC, AVANTA Σ) coupled to flame ionization. The Temperature Programmed Reduction ($H_2$-TPR) was carried out with a ChemBET Pulsar TPR/TPD equipment from Quantachrome instruments following the $H_2$ consumption by TCD. The textural morphology of the materials was studied by Scanning Electronic Microscopy (SEM) (JEOL, JSM-6490LV) and Transmission Electronic Microscopy (TEM) (Tecnai F20 Super Twin TMP of FEI). X-Ray Diffraction (XRD) was carried out with a PANalytical X'Pert PRO MRD equipment. Thermogravimetric Analysis (TGA) was performed using a TGA1-Mettler Toledo equipment.

### *Catalyst test*

The catalytic tests of CO-PROX were carried out in a U-shaped reactor connected online to a gas chromatograph (Hewlett Packard 5890 Series A) with a packed molecular sieve 13X column, and a TCD at 0,76 atm pressure. The temperature was controlled using a cylindrical shape furnace with a thermocouple in the center of the system close to the catalytic fixed-bed. The samples were submitted to an oxidant atmosphere treatment for 1 h at 300 °C. The reaction gas feed consisted of 2 % vol. CO, 2 % vol. $O_2$, 50 % vol. $H_2$ with He as gas balance, and a total flow rate of 100 mL/min, through 100 mg of the catalyst with 60-80 mesh. The corresponding space velocity is 60 000 mL $g^{-1}$ $h^{-1}$. The content of $CO_2$ and $H_2O$ in the reaction stream was limited to 2 % vol. and 3 % vol., respectively, instead of 10-20 % vol. (real content), due to the experimental restrictions of the catalytic reaction system. However, this amount was enough to observe the kinetic inhibition effect by competitive adsorption in the CO-PROX reaction (Córdoba and Martínez-Hernández, 2015).

In this study, the catalytic test consisted of four steps. In step I, the bimetallic catalysts Au-$CuO_x$/CeZr and Au/CuCeZr were evaluated in the CO-PROX and the best catalytic performance, Au-$CuO_x$/CeZr, was compared with the monometallic catalysts Au/CeZr and $CuO_x$/CeZr. In step II and III, the $CO_2$ and $H_2O$ effect of Au-$CuO_x$/CeZr bimetallic catalyst was evaluated, considering that both compounds can be produced in the reforming process for hydrogen production (Cobo et al., 2013; Tippawan and Arpornwichanop, 2014). Finally, in step IV, the catalytic stability test was performed on Au-$CuO_x$/CeZr bimetallic catalyst for 118 h at the temperature with the major activity, with $CO_2$ and water in the feed effluent.

The CO conversion ($X_{CO}$) and selectivity to $CO_2$ ($S_{CO_2}$) were calculated using Equation (1) and Equation (2), respectively.

$$X_{CO}(\%) = \frac{F_{CO,initial} - F_{CO,final}}{F_{CO,initial}} \times 100 \quad (1)$$

$$S_{CO_2}(\%) = \frac{F_{CO,initial} - F_{CO,final}}{2 \times (F_{O_2,initial} - F_{O_2,final})} \times 100 \quad (2)$$

where $F_{CO,initial}$ and $F_{O_2,initial}$ are the molar flows of CO and $O_2$ in the feed stream, and $F_{CO,final}$ and $F_{O_2,final}$ are the molar flows in the outlet stream.

## Results and discussion

### *$N_2$ adsorption-desorption isotherms*

Table 1 presents the BET specific area and the composition percentages of the metals loaded in the catalytic materials. The quantified experimental values agree with the theoretical values (2 % and 4 % w/w for gold and copper, respectively) indicating that the synthesis methods are suitable for obtaining reproducible catalytic materials.

The isotherms for the bimetallic catalytic materials, which are not shown here, were type IV, typical of mesoporous materials (Thommes et al., 2015), with a H2 hysteresis, related to the not well-defined distribution of pore shape materials (Thommes, 2007).

It is evident that incorporated copper samples showed the lowest specific area, and that mono and bimetallic samples present a lower surface area than support materials. The inclusion of copper ions in Cerium-Zirconium mixed oxides modifies the crystalline structure and the presence of Au, $CuO_x$ and Au-$CuO_x$ facilitates the obstruction of the smaller porous, which results in a lower surface area compared with the supports (Gurbani et al., 2009).

In the case of Au-$CuO_x$/CeZr bimetallic catalyst, the surface area is slightly lower than Au/CeZr sample but higher than $CuO_x$/CeZr. This behavior can be related to a higher dispersion of the $CuO_x$ derived from the interaction with gold, avoiding the subsequent porous obstructions.

**Table 1.** Chemical composition and BET specific area of supports, bimetallic and monometallic samples

| Sample | BET surface area ($m^2$/g) | %Au (%w/w) | %Cu (%w/w) |
|---|---|---|---|
| CeZr | 28 | – | – |
| Au/CeZr | 22 | 2,2 | – |
| $CuO_x$/CeZr | 11 | – | 3,0 |
| Au-$CuO_x$/CeZr | 19 | 1,9 | 4,1 |
| CuCeZr | 3 | – | 3,8 |
| Au/CuCeZr | 2 | 1,8 | 3,7 |

**Source:** Authors

### *Temperature programmed reduction (TPR-$H_2$)*

Figure 1 presents the TPR-$H_2$ patterns of the supports and the catalytic samples. Due to the limitations of the TPR test, results were only analyzed qualitatively.

The reduction profile of Cerium-Zirconium support (not shown) is characterized by a wide peak at about 563 °C, which is attributed to the strong interaction between $CeO_2$ and $ZrO_2$ and the solid solution obtained (Córdoba and Martínez-Hernández, 2015).

The Au/CeZr reduction pattern shows two hydrogen consumption peaks around 170 and 240 °C, which are related to the reduction of $Au^{3+}$ species, promoting slightly the $H_2$ spillover phenomenon and therefore the cerium reduction at lower temperature (Fonseca et al., 2012; Laguna et al., 2014).

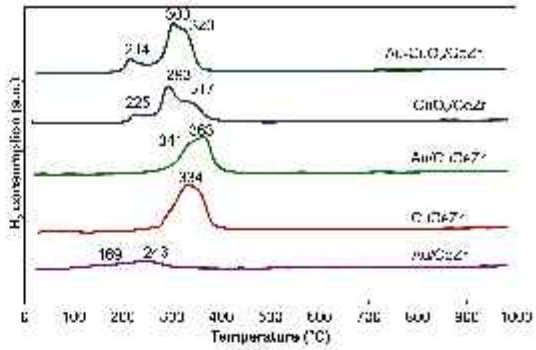


**Figure 1.** TPR-$H_2$ patterns of the bimetallic catalysts Au-$CuO_x$/CeZr, Au/CuCeZr; the monometallic catalysts $CuO_x$/CeZr, CuCeZr, Au/CeZr; and the CeZr support.
**Source:** Authors

The TPR profiles for $CuO_x$/CeZr and Au-$CuO_x$/CeZr are similar, showing three reduction peaks (Figure 1) at around 220, 300 and 320 °C, indicating no strong effect of gold on the cerium reduction temperatures. The first peak correspond to the reduction of copper clusters with lower oxidation, the next peak to the reduction of isolated copper species with higher oxidation state and the last peak to the simultaneous reduction of copper and surface cerium oxide (Gurbani et al., 2009; Liao, Chu, Dai and Pitchon, 2013; Martínez-Arias et al., 2009).

The samples with incorporated copper (CuCeZr, Au/CeZr) present two reduction peaks at slightly higher temperatures than CeZr based samples, indicating a more difficult reduction for copper. The reduction peaks of incorporated copper samples can be attributed to the simultaneous reduction of highly dispersed species ($Cu^{2+}$ to $Cu^{1+}$) in strong interaction with the support, and the superficial $Ce^{4+}$ reduction in the interface Cu-$CeO_2$ (Araújo, Bellido, Bernardi, Assaf and Assaf, 2012; Reina et al., 2016).

### *Textural morphology*

The morphology of the catalytic materials was evaluated by Scanning Electron Microscopy (SEM) and Transmission Electron Microscopy (TEM). Figure 2 presents the SEM of the bimetallic catalysts.

The SEM results show that the catalyst Au-$CuO_x$/CeZr presented smaller particles formation on the larger particles of the material, while the Au/CuCeZr did not generate this type of particle. The formation of smaller particles can be attributed to the presence of $CuO_x$ on the bimetallic catalyst with impregnated copper (Au-$CuO_x$/CeZr). Figure 3 presents the TEM results of the bimetallic catalysts.

The formation of circular particles was promoted in the bimetallic catalyst with impregnated copper (Au-$CuO_x$/CeZr). However, the presence of well-defined nano-gold particles was not observed, possibly due to the masking effect of the copper oxide or the agglomeration of gold particles in the calcination step.

For the bimetallic catalyst with incorporated copper (Au/CuCeZr), particles of around 4 nm are observed. EDX

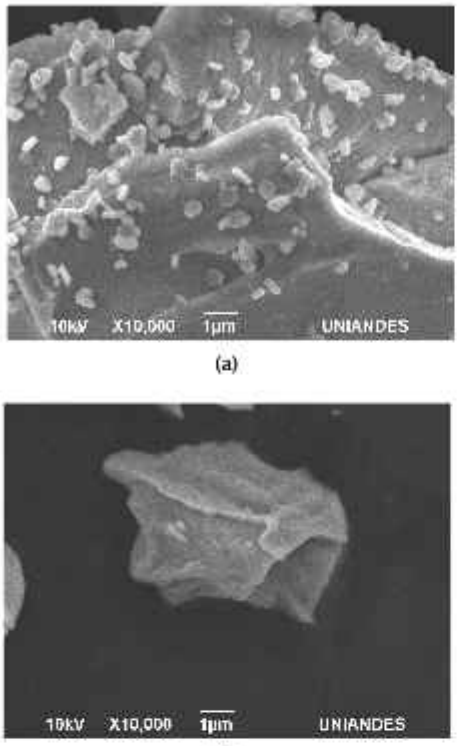


**Figure 2.** SEM micrographs: (a) Au-$CuO_x$/CeZr and (b) Au/CuCeZr.
**Source:** Authors

analysis and a closer micrograph are required to confirm the chemical nature of the particles, since the one presented in Figure 3 does not allow an undoubted differentiation of gold, taking into account the nature of the support.

## *X-Ray Diffraction*

Figure 4 presented the XRD patterns for the bimetallic catalysts. The materials presented diffraction peaks corresponding to the fluorite cubic structure of the mixed oxide cerium-zirconium, which is identified by the planes (1 1 1), (2 0 0), (2 2 0), (2 2 0), and (4 0 0) (JCPDS Card No. 28-0271), with an incorporation of $ZrO_2$ in the $CeO_2$ lattice forming a homogenous solid solution (Biswas and Kunzru, 2007; Córdoba and Martínez-Hernández, 2015).

Table 2 presents the average crystallite size and the lattice parameter (a) from XRD peak positions and indexation. The bimetallic catalysts did not present changes in the fluorite cubic crystalline structure when gold and copper are added. The position of peaks in both bimetallic catalysts shifted slightly toward high angles with respect to the support, which is in accordance with the decrease in the lattice parameter of bimetallic catalysts due to a possible interaction between the copper and the fluorite CeZr structure. This is not due to an insertion of copper in the crystalline structure forming a true solid solution, but to a high copper dispersion into the mixed oxides solution (Marban and Fuertes 2005).

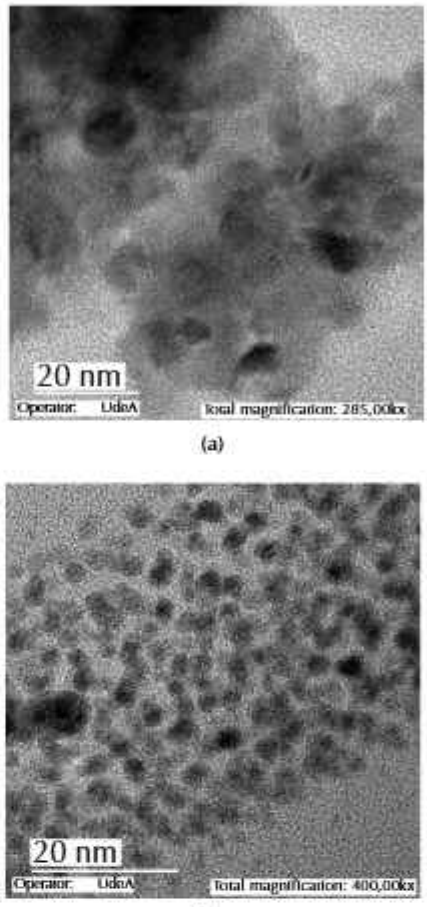


**Figure 3.** TEM micrographs: (a) Au-$CuO_x$/CeZr and (b) Au/CuCeZr.
**Source:** Authors

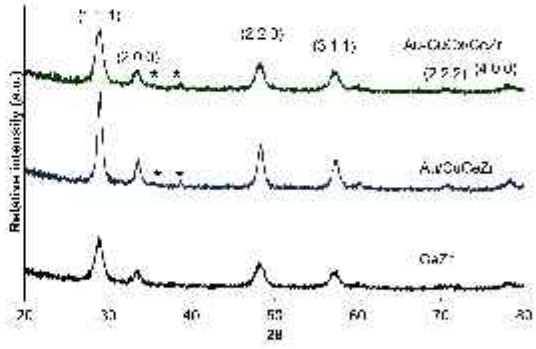


**Figure 4.** XRD patterns of CeZr support and the catalysts Au-$CuO_x$/CeZr and Au/CuCeZr *CuO.
**Source:** Authors

Signals corresponding to gold did not present patterns in XRD in the bimetallic catalyst (Figure 4), since gold percentage (about 2% w/w) is too low for being detected by XRD patterns. Additionally, it has been reported that gold particles below 5 nm cannot be detected by XRD (Ilieva et al., 2009; Reina, Ivanova, Centeno and Odriozola, 2014), which is in accordance with TEM results.

**Table 2.** Structural parameters of the catalyst materials

| Sample | Average crystallite size, d(nm)* | Lattice parameter, a (Å) |
|---|---|---|
| CeZr | 17,1 | 5,354 |
| Au/CeZr | 17,1 | 5,342 |
| $CuO_x$/CeZr | 15,7 | 5,358 |
| Au-$CuO_x$/CeZr | 15,9 | 5,316 |
| CuCeZr | 22,4 | 5,339 |
| Au/CuCeZr | 22,4 | 5,318 |

*Calculated with the Scherrer equation of the plane (1 1 1)

**Source:** Authors

However, diffraction peaks 35,5° and 38,7° correspond to the cluster of copper oxide, such as tenorite (Moretti et al., 2015). These CuO signals were present in the bimetallic catalyst with impregnated copper (Au-$CuO_x$/CeZr) and in the bimetallic catalyst with incorporated copper (Au/CuCeZr), discarding the formation of the solid solution Au-Cu (Laguna et al., 2014).

The TGA was done in the bimetallic catalyst with impregnated copper (Au-$CuO_x$/CeZr) before and after CO-PROX stability reaction test to determine coke formation (not shown). Results did not show weight loss in this temperature range, which suggests that the bimetallic catalyst used Au-$CuO_x$/CeZr present no carbonaceous deposits formation.

## *Catalytic test*

- Step I

Figure 5 presents the results of the CO conversion and $CO_2$ selectivity of both bimetallic catalysts.

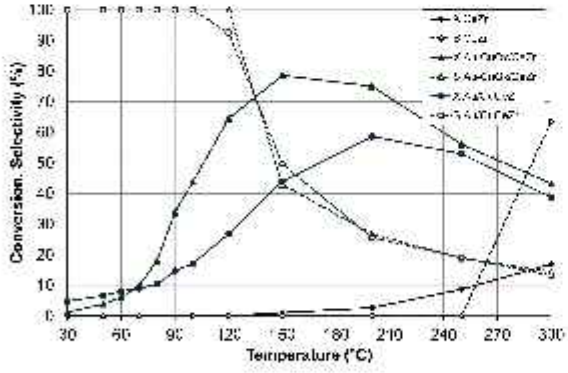


**Figure 5.** CO conversion (X, filled symbols) and selectivity to $CO_2$ (S, empty symbols) of CeZr, Au-$CuO_x$/CeZr and Au/CuCeZr. Feed stream: 2 % CO, 2 % $O_2$, 50 % $H_2$ and He (balance).
**Source:** Authors

The Au-$CuO_x$/CeZr presented a better behavior with respect to the Au/CuCeZr due to the possible effect of copper in the CO-PROX activity. Cu-Ce interactions in the catalyst by wet impregnation promote the formation of large interfaces Cu-Ce, where CO is absorbed to oxidation. It is believed that the reaction is catalyzed by the interfacial copper oxide–ceria centers in which ceria presents a high number of oxygen vacancies that allows high mobility of lattice oxygen (Marbán and Fuertes, 2005).

The higher catalytic activity of the Au-$CuO_x$/CeZr with respect to the Au/CuCeZr is in agreement with TPR-$H_2$ results, where the Au-$CuO_x$/CeZr presented a higher reducibility to lower temperatures than the Au/CuCeZr. Additionally, the Au/CuCeZr presented a lower surface area.

The catalytic behavior of the Au-$CuO_x$/CeZr might be related to the formation of smaller particles on the large particles of the material (SEM results), as well as to the good size distribution of particles of about 5 nm (TEM results). The Au/CuCeZr favored the formation of nanoparticles of 4 nm (TEM results). However, the gold activity was inhibited with the incorporation of copper.

Figure 6 presents the CO conversion and selectivity to $CO_2$ of the Au-$CuO_x$/CeZr with respect to the monometallic catalyst of gold (Au/CeZr) and impregnated copper ($CuO_x$/CeZr).

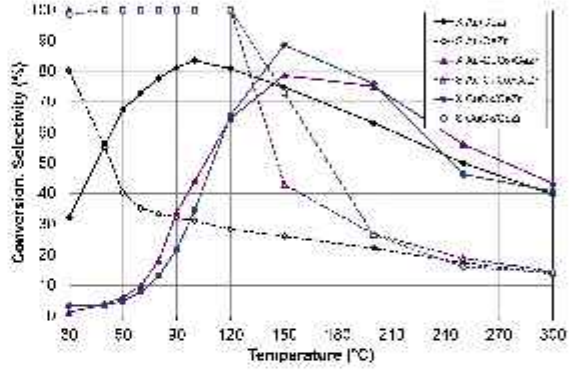


**Figure 6.** CO conversion (X, filled symbols) and selectivity to $CO_2$ (S, empty symbols) of Au-$CuO_x$/CeZr with respect to Au/CeZr and $CuO_x$/CeZr. Feed stream: 2 % CO, 2 % $O_2$, 50 % $H_2$ and He (balance).
**Source:** Authors

The bimetallic catalyst Au-$CuO_x$/CeZr (Figure 6) showed the best catalytic performance, since the CO conversion curve volcano-type was wider than in the monometallic catalyst of gold (Au/CeZr) and impregnated copper ($CuO_x$/CeZr). Although $CuO_x$/CeZr had the highest CO conversion, the bimetallic catalyst provided greater stability throughout the evaluated temperatures. The good activity can be related to the bimetallic interaction, i.e. the formation of a cooper monolayer on gold plates, which allows the adsorption/activation of $O_2$ and the formation of $CO_2$ through CO and O coadsorption. This favored the formation of alloy active sites that participate in the CO oxidation and increase the reaction speed (Hussain, 2013). The selectivity of the Au-$CuO_x$/CeZr was enhanced with respect to the monometallic catalyst Au/CeZr. To establish the bimetallic interaction, further experiments with techniques such as HR-TEM and XPS are needed.

The bimetallic catalyst of impregnated copper Au-$CuO_x$/CeZr presented a better catalytic performance than Au/CuCeZr, therefore the Au-$CuO_x$/CeZr was selected for the evaluation of the next step.

- Step II

Figure 7 presents the results of the CO conversion and the selectivity to $CO_2$ of bimetallic catalyst with incorporated copper (Au-$CuO_x$/CeZr), evaluating the effect of $CO_2$ in the CO-PROX.

The addition of $CO_2$ in the feed effluent affected the catalytic activity of Au-$CuO_x$/CeZr, since it required a higher temperature to reach the maximum conversion (Figure 7). The bimetallic catalyst presented a slightly lower activity than the same catalyst evaluated without $CO_2$. The selectivity was not affected by the $CO_2$ addition. Laguna et al. (2014) reported that the presence of $CO_2$ decreases CO conversion below 150 °C due to the competence in the adsorption between CO and $CO_2$.

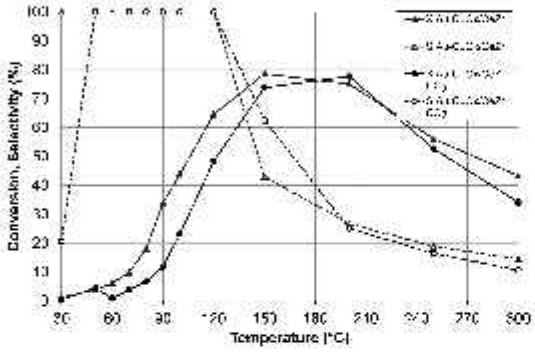


**Figure 7.** Effect of $CO_2$ on the CO conversion (X, filled symbols) and selectivity to $CO_2$ (S, empty symbols) of Au-$CuO_x$/CeZr. Feed stream: 2 % CO, 2 % $O_2$, 2 % $CO_2$, 50 % $H_2$ and He (balance).
**Source:** Authors

- Step III

Figure 8 presents the results of CO conversion and selectivity to $CO_2$ of Au-CuOx/CeZr, evaluating the effect of water and $CO_2$ addition in the feed stream.

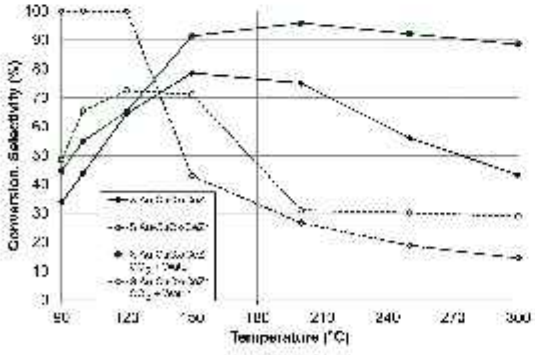


**Figure 8.** Effect of water and $CO_2$ on the CO conversion (X, filled symbols) and selectivity to $CO_2$ (S, empty symbols) of Au-CuOx/CeZr. Feed stream: 2 % CO, 2 % $O_2$, 2 % $CO_2$, 3 % $H_2O$, 50 % $H_2$ and He (balance).
**Source:** Authors

The reaction feed mixture was humidified by bubbling it through a container of deionized water at room temperature, yielding 2 % water vapor in the gas fed to the reactor. The addition of water in the feed effluent had a positive effect on the bimetallic catalyst (Figure 8), increasing CO conversion with respect to bimetallic catalyst without $CO_2$ and water. Au-$CuO_x$/CeZr presented a conversion above 90 % between 150 and 300 °C. The catalyst achieved a maximum conversion of 96 % at 200 °C. The selectivity was better with water addition, even though it was inhibited below 120 °C.

The favorable effect of water on the activity of the bimetallic catalyst can be explained by the formation of hydroxide groups in the dissociative adsorption of water on the active sites of gold (Liao et al., 2013; Mozer et al., 2009). The presence of $CO_2$ and $H_2O$ can also affect the catalytic behavior of the monometallic catalyst since a competitive adsorption is expected and therefore an effect on the activity and selectivity. Further studies are needed in order to confirm this effect.

- Step IV

Figure 9 presents the results of the catalytic stability of Au-$CuO_x$/CeZr, evaluating CO conversion and selectivity to $CO_2$ with the addition of water and $CO_2$ in the feed effluent.

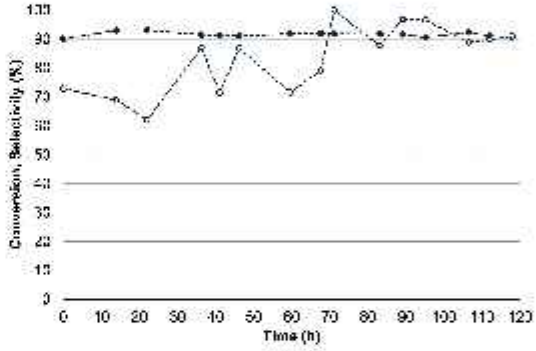


**Figure 9.** Catalytic stability of the Au-CuOx/CeZr. Evaluation of the CO conversion (X, filled symbols) and selectivity to $CO_2$ (S, empty symbols) with addition of $CO_2$ and water. Feed stream: 2 % CO, 2 % $O_2$, 2 % $CO_2$, 3 % $H_2O$, 50 % $H_2$ and He (balance).
**Source:** Authors

The bimetallic catalyst Au-$CuO_x$/CeZr presented a good behavior in the stability test, with was stable for 118 h, obtaining CO conversion of 92 % and selectivity of 90 %, representing an ooutstanding performance. Fonseca, Ferreira et al. (2012) evaluated a bimetallic catalyst Au-Cu over $CeO_2$ in the presence of 10 vol. % of $CO_2$ and 2 vol % of $H_2O$, and reached a CO conversion of 60 % and a selectivity of 85 % during 8 h without deactivation. However, since the feed compositions evaluated in this work are quite different than those tested by Fonseca, Ferreira et al., the differences in the catalytic behavior could be related to the important role of these compounds.

## Conclusions

All the samples presented the crystalline fluorite-type structure, with the presence of CuO in the monometallic

and bimetallic materials with copper, enhancing the catalytic activity. It was possible to obtain nano-gold particles that promoted catalytic behavior.

The bimetallic catalyst with impregnated copper (Au-$CuO_x$/CeZr) and the bimetallic catalyst with copper incorporated (Au/CuCeZr) were evaluated in the CO-PROX. Results showed that the bimetallic catalyst with impregnated copper presented the best catalytic performance, since it exhibited high activity, good selectivity and good long-term stability throughout the evaluated temperatures, even in the presence of $CO_2$ and $H_2O$ in the feed stream.

The Au-$CuO_x$/CeZr catalyst presents a cooperative effect between gold and copper, promoting higher stability in the catalytic activity, CO conversion and selectivity to $CO_2$ in the evaluated temperature window. Au and Cu interaction promotes the redox properties of the CeZr mixed oxide allowing the reduction of $Ce^{4+}$ ions to lower temperatures and improving the redox behavior.

## Acknowledgements

The authors are grateful to the Universidad Nacional de Colombia - Campus Bogotá for the financial support of this work.

## References

Araújo, V. D., Bellido, J. D. , Bernardi, M. I. B., Assaf, J. M., and Assaf, E. M. (2012). CuO-$CeO_2$ catalysts synthesized in one-step: Characterization and PROX performance. *International Journal of Hydrogen Energy*, *37*(7), 5498-5507. DOI: 10.1016/j.ijhydene.2011.12.143

Avgouropoulos, G., Ioannides, T., Papadopoulou, C., Batista, J., Hocevar, S., and Matralis, H. K. (2002). A comparative study of Pt/$\gamma$-$Al_2O_3$, Au/$\alpha$-$Fe_2O_3$ and CuO-$CeO_2$ catalysts for the selective oxidation of carbon monoxide in excess hydrogen. *Catalysis Today*, *75*(1-4), 157-167. DOI: 10.1016/S0920-5861(2)00058-5

Biswas, P., and Kunzru, D. (2007). Steam reforming of ethanol for production of hydrogen over Ni/$CeO_2$-$ZrO_2$ catalyst: Effect of support and metal loading. *International Journal of Hydrogen Energy*, *32*, 969-980. DOI: 10.1016/j.ijhydene.2006.09.031

Biswas, P., and Kunzru, D. (2008). Oxidative steam reforming of ethanol over Ni/$CeO_2$-$ZrO_2$ catalyst. *Chemical Engineering Journal*, *136*, 41-49. DOI: 10.1016/ j.cej.2007.03.057

Cheng, X., Shi, Z., Glass, N., Zhang, L., Zhang, J., Song, D., Shen, J. (2007). A review of PEM hydrogen fuel cell contamination: Impacts, mechanisms, and mitigation. *Journal of Power Sources*, *165*(2), 739-756. DOI: 10.1016/ j.jpowsour.2006.12.012

Choudhary, T. V., and Goodman, D. W. (2002). CO-Free Fuel Processing for Fuel Cell Applications. *Catalysis Today*, *77*(1-2), 65-78. DOI: 10.1016/S0920-5861(2)00233-X

Cobo, M., Pieruccini, D., Abello, R., Ariza, L., Córdoba, L. F., and Conesa, J. A. (2013). Steam reforming of ethanol over bimetallic RhPt/$La_2O_3$: Long-term stability under favorable reaction conditions. *International Journal of Hydrogen Energy*, *38*, 5580-5593. DOI: 10.1016/ j.ijhydene.2013.02.044

Córdoba, L. F., and Martínez-Hernández, A. (2015). Preferential oxidation of CO in excess of hydrogen over Au/$CeO_2$-$ZrO_2$ catalysts. *International Journal of Hydrogen Energy*, *40*(46), 16192-16201. DOI: 10.1016/ j.ijhydene.2015.09.133

Das, D., Llorca, J., Colussi, S., Dominguez, M., Colussi, S., Trovarelli, A., and Gayen, A. (2015). Methanol steam reforming behavior of copper impregnated over $CeO_2$-$ZrO_2$ derived from a surfactant assisted coprecipitation route. *International Journal of Hydrogen Energy*, *40*(33), 10463-10479. DOI: 10.1016/j.ijhydene.2015.06.130

Di Benedetto, A., Landi, G., and Lisi, L. (2018). Catalysts by Using Nanometric Ceria as Support. *Catalysts*, *8*(209), 1-19. DOI: 10.3390/catal8050209

Epling, W. S., Cheekatamarla, P. K., and Lane, A. M. (2003). Reaction and surface characterization studies of titania-supported Co, Pt and Co/Pt catalysts for the selective oxidation of CO in $H_2$-containing streams. *Chemical Engineering Journal*, *93*(1), 61-68. DOI: 10.1016/S1385-8947(2)00109-2

Fonseca, J., Ferreira, H. S., Bion, N., Pirault-Roy, L., Rangel, M. D. C., Duprez, D., and Epron, F. (2012). Cooperative effect between copper and gold on ceria for CO-PROX reaction. *Catalysis Today*, *180*(1), 34-41. DOI: 10.1016/ j.cattod.2011.06.008

Fonseca, J., Royer, S., Bion, N., Pirault-Roy, L., Rangel, M. do C., Duprez, D., and Epron, F. (2012). Preferential CO oxidation over nanosized gold catalysts supported on ceria and amorphous ceria-alumina. *Applied Catalysis B, Environmental*, *128*, 10-20. DOI: 10.1016/ j.apcatb.2012.03.037

Gurbani, A., Ayastuy, J. L., Gonzàlez-Marcos, M. P., Herrero, J. E., Guil, J. M., and Gutièrrez-Ortiz, M. A. (2009). Comparative study of CuO-$CeO_2$ catalysts prepared by wet impregnation and deposition-precipitation. *International Journal of Hydrogen Energy*, *34*(1), 547-553. DOI: 10.1016/ j.ijhydene.2008.10.047

Haruta, M. (2002). Catalysis of gold nanoparticles deposited on metal oxides. *CATTECH*, *6*(3), 102-115. DOI: 10.1023/ A:1020181423055

Haruta, M., Kobayashi, T., Sano, H., and Yamada, N. (1987). Novel Gold Catalysts for the Oxidation of Carbon Monoxide at a Temperature far Below 0 °C. *Chemistry Letters*, *16*(2) 405-408. DOI: 10.1246/cl.1987.405

Haryanto, A., Fernando, S., Murali, N., and Adhikari, S. (2005). Current status of hydrogen production techniques by steam reforming of ethanol: A review. *Energy and Fuels*, *19*(5), 2098-2106. DOI: 10.1021/ef0500538

Hussain, A. (2013). Beneficial Effect of Cu on a Cu-Modified Au Catalytic Surface for CO Oxidation Reaction?: A DFT Study. *The Journal of Physical Chemistry*, *117*(10), 5084-5094. DOI: 10.1021/jp3111887

Ilieva, L., Pantaleo, G., Ivanov, I., Zanella, R., Venezia, A. M., and Andreeva, D. (2009). A comparative study of differently prepared rare earths-modified ceria-supported gold catalysts for preferential oxidation of CO. *International Journal of Hydrogen Energy*, *34*(15), 6505-6515. DOI: 10.1016/j.ijhydene.2009.05.141

Ko, E. Y., Park, E. D., Seo, K. W., Lee, H. C., Lee, D., and Kim, S. (2006). A comparative study of catalysts for the preferential CO oxidation in excess hydrogen. *Catalysis Today*, *116*(3), 377-383. DOI: 10.1016/j.cattod.2006.05.072

Kosmambetova, G. R., Moroz, E. M., Guralsky, A.V., Pakharukova, V. P., Boronin, A. I., Ivashchenko, T. S., Strizhak, P. E. (2011). Low temperature hydrogen purification from CO for fuel cell application over copper-ceria catalysts supported on different oxides. *International Journal of Hydrogen Energy*, *36*(1), 1271-1275. DOI: 10.1016/j.ijhydene.2010.06.126

Laguna, O. H., Centeno, M. A., Arzamendi, G., Gandía, L. M., Romero-Sarria, F., and Odriozola, J. A. (2010). Iron-modified ceria and Au/ceria catalysts for total and preferential oxidation of CO (TOX and PROX). *Catalysis Today*, *157*(1-4), 155-159. DOI: 10.1016/j.cattod.2010.04.011

Laguna, O. H., Hernández, W. Y., Arzamendi, G., Gandía, L. M., Centeno, M. A., and Odriozola, J. A. (2014). Gold supported on $CuO_x/CeO_2$ catalyst for the purification of hydrogen by the CO preferential oxidation reaction (PROX). *Fuel*, *118*, 176-185. DOI: 10.1016/ j.fuel.2013.10.072

Laguna, O. H., Ngassa, E. M., Oraá, S., Alvarez, A., Domínguez, M. I., Romero-Sarria, F., Odriozola, J. A. (2012). Preferential oxidation of CO (CO-PROX) over $CuO_x/CeO_2$ coated microchannel reactor. *Catalysis Today*, *180*(1), 105-110. DOI: 10.1016/j.cattod.2011.03.024

Li, X., Fang, S. S. S., Teo, J., Foo, Y.L., Borgna, A., Lin, M. and Zhong, Z. (2012). Activation and Deactivation of Au-Cu/SBA-15 Catalyst for Preferential Oxidation of CO in $H_2$-Rich Gas. *ACS Catalysis*, *2*(3), 360-369. DOI: 10.1021/cs200536a

Liao, X., Chu, W., Dai, X., and Pitchon, V. (2013). Bimetallic Au–Cu supported on ceria for PROX reaction?: Effects of Cu/Au atomic ratios and thermal pretreatments. *Applied Catalysis B, Environmental*, *142-143*, 25-37. DOI: 10.1016/j.apcatb.2013.05.010

Lin, J., and Wan, B. (2003). Effects of preparation conditions on gold/Y-type zeolite for CO oxidation. *Applied Catalysis B: Environmental*, *41*(1-2), 83-95. DOI: 10.1016/S0926-3373(2)00195-9

Liu, W., and Flytzanistephanopoulos, M. (1995). Total Oxidation of Carbon Monoxide and Methane over Transition Metal Fluorite Oxide Composite Catalysts: I. Catalyst Composition and Activity. *Journal of Catalysis*, *153*(2), 304-316. DOI: 10.1006/jcat.1995.1132

Liu, X., Wang, A., Zhang, T., Su, D. S., and Mou, C. Y. (2011). Au-Cu alloy nanoparticles supported on silica gel as catalyst for CO oxidation: Effects of Au/Cu ratios. *Catalysis Today*, *160*(1), 103-108. DOI: 10.1016/j.cattod.2010.05.019

Manzolini, G., and Tosti, S. (2008). Hydrogen production from ethanol steam reforming: energy efficiency analysis of traditional and membrane processes. *International Journal of Hydrogen Energy*, *33*R, 5571-5582. DOI: 10.1016/j.ijhydene.2008.06.029

Marbán, G., and Fuertes, A. B. (2005). Highly active and selective $CuO_x/CeO_2$ catalyst prepared by a single-step citrate method for preferential oxidation of carbon monoxide, *57*(1), 43-53. DOI: 10.1016/j.apcatb.2004.10.011

Mariño, F., Baronetti, G., Laborde, M., Bion, N., Le Valant, A., Epron, F., and Duprez, D. (2008). Optimized CuO-$CeO_2$ catalysts for COPROX reaction. *International Journal of Hydrogen Energy*, *33*(4), 1345-1353. DOI: 10.1016/j.ijhydene.2007.12.014

Martínez-Arias, A., Fernández-García, M., Hungría, A. B., Iglesias-Juez, A., Gálvez, O., Anderson, J. A., Munuera, G. (2003). Redox interplay at copper oxide-$(Ce,Zr)O_x$ interfaces: Influence of the presence of NO on the catalytic activity for CO oxidation over CuO/$CeZrO_4$. *Journal of Catalysis*, *214*(2), 261-272. DOI: 10.1016/S0021-9517(2)00084-2

Martínez-Arias, A., Gamarra, D., Fernández-García, M., Hornés, A., Bera, P., Koppány, Z., and Schay, Z. (2009). Redox-catalytic correlations in oxidised copper-ceria CO-PROX catalysts. *Catalysis Today*, *143*(3-4), 211-217. DOI: 10.1016/j.cattod.2008.09.018

Martínez-Arias, A., Hungría, A. B., and Munuera, G. (2006). Preferential oxidation of CO in rich $H_2$ over CuO/$CeO_2$: Details of selectivity and deactivation under the reactant stream, *Applied Catalysis B: Environmental*, *65*(3-4), 207-216. DOI: 10.1016/j.apcatb.2006.02.003

Moretti, E., Storaro, L., Talon, A., Riello, P., Infantes, A., and Rodríguez-Castellón, E. (2015). 3-D flower like Ce-Zr-Cu mixed oxide systems in the CO preferential oxidation (CO-PROX): Effect of catalyst composition. *Applied Catalysis B, Environmental*, *168-169*, 385-395. DOI: 10.1016/j.apcatb.2014.12.032

Mozer, T. S., Dziuba, D. A., Vieira, C. T. P., and Passos, F. B. (2009). The effect of copper on the selective carbon monoxide oxidation over alumina supported gold catalysts. *Journal of Power Sources*, *187*(1), 209-215. DOI: 10.1016/j.jpowsour.2008.10.068

Ocampo, F., Louis, B., and Roger, A.-C. (2009). Methanation of carbon dioxide over nickel-based $Ce_{0.72}Zr_{0.28}O_2$ mixed oxide catalysts prepared by sol-gel method. *Applied Catalysis A: General*, *369*, 90-96. DOI: 10.1016/j.apcata.2009.09.005

Reina, T. R., Ivanova, S., Centeno, M. A., and Odriozola, J. A. (2014). Catalytic screening of Au/$CeO_2$-$MO_x/Al_2O_3$ catalysts (M = La, Ni, Cu, Fe, Cr, Y) in the CO-$PrO_x$ reaction. *International Journal of Hydrogen Energy*, *40*, 1782-1788. DOI: 10.1016/j.ijhydene.2014.11.141

Reina, T. R., Ivanova, S., Laguna, O. H., Centeno, M. A., and Odriozola, J. A. (2016). WGS and CO-$PrO_x$ reactions using gold promoted copper-ceria catalysts: "bulk CuO-$CeO_2$ vs. CuO-$CeO_2/Al_2O_3$ with low mixed oxide content". *Applied Catalysis B: Environmental*, *197*, 62-72. DOI: 10.1016/j.apcatb.2016.03.022

Salemme, L., Menna, L., Simeone, M., and Volpicelli, G. (2010). Energy efficiency of membrane-based fuel processors - PEM fuel cell systems. *International Journal of Hydrogen Energy*, *35*(8), 3712-3720. DOI: 10.1016/ j.ijhydene.2010.01.096

Thommes, M. (2007). Textual Characterization of Zeolites and Ordered Mesoporous Materials by Physical Adsorption. In J. Čejka, H. van Bekkum, A. Cormo, and F. Schüth (Eds.), *Introduction to Zeolite Science and Practice*. Volume 168 (3nd ed.). Elsevier B. V.

Thommes, M., Kaneko, K., Neimark, A. V., Olivier, J. P., Rodriguez-Reinoso, F., Rouquerol, J., and Sing, K. S. W. (2015). Physisorption of gases, with special reference to the evaluation of surface area and pore size distribution (IUPAC Technical Report). *Pure and Applied Chemistry*, *87*(9-10), 1051-1069. DOI: 10.1515/pac-2014-1117

Tippawan, P., and Arpornwichanop, A. (2014). Energy and exergy analysis of an ethanol reforming process for solid oxide fuel cell applications. *Bioresource Technology*, *157*, 231-239. DOI: 10.1016/j.biortech.2014.01.113

Trovalleri, A. (Ed.). (2002). *Catalysis by Ceria and Related Materials*. London: Imperial College Press.

Vargas, J. C., Libs, S., Roger, A.-C., and Kiennemann, A. (2005). Study of Ce-Zr-Co fluorite-type oxide as catalysts for hydrogen production by steam reforming of bioethanol. *Catalysis Today*, *107-108*, 417-425. DOI: 10.1016/ j.cattod.2005.07.118

Zhu, C., Ding, T., Gao, W., Ma, K., Tian, Y., and Li, X. (2017). $CuO/CeO_2$ catalysts synthesized from Ce-UiO-66 metal-organic framework for preferential CO oxidation. *International Journal of Hydrogen Energy*, *42*(27), 17457-17465. DOI: 10.1016/j.ijhydene.2017.02.088

Juan David Arévalo, Julio César Vargas,
Luis Fernando Córdoba

**Effect of the presence of $CuO_x$ on the catalytic behavior of bimetallic Au-Cu catalyst supported on Ce-Zr mixed oxide in CO preferential oxidation**
**Influencia de la presencia de $CuO_x$ sobre el comportamiento catalítico de un catalizador bimetálico Au-Cu soportado en óxido mixto Ce-Zr en la oxidación preferencial de CO**

*Ingeniería e Investigación*
vol. 39, no. 2, p. 21 - 30, 2019
Facultad de Ingeniería, Universidad Nacional de Colombia.,
**ISSN:** 0120-5609
**ISSN-E:** 2248-8723

**DOI:** https://doi.org/10.15446/ing.investig.v39n2.76586